Applied Biological Research 27(1): 137-146; (2025)
DOI: 10.48165/abr.2025.27.01.13

MYCOGENIC PRODUCTION OF MAGNESIUM NANOPARTICLES FOR ANTIFUNGAL ACTIVITY AGAINST *Alternaria mali* INFECTING APPLE (*Malus x domestica*)

Shahnaz Anjum[1], Tariq Ahmad Sofi[2*], Ashish Vyas[3] and Arfa Ji[4]

[1]*Department of Botany,* [3]*Department of Microbiology, LPU, Phagwara - 144 411, Punjab (India)*
[2]*Division of Plant Pathology, Faculty of Horticulture, SK University of Agricultural Sciences & Technology-Kashmir, Shalimar, Srinagar - 190 025, Jammu & Kashmir (India)*
[4]*Department of Biotechnology, University of Kashmir, Srinagar – 190 006, Jammu & Kashmir (India)*
*****e-mail: *tariqsofi1@gmail.com*

ABSTRACT

The potential of magnesium oxide nanoparticles (MgONP) as a new and efficient bio-fungicide against apple plant pathogen *Alternaria mali* was assessed. The study was carried out to synthesize MgONP's from *Pleurotus sajor-caju* cell filtrate, and characterize them by UV-visible spectroscopy, scanning electron microscopy, Energy-dispersive X-ray spectroscopy, X-ray diffraction, particle size analysis and Fourier transform infra-red spectroscopy (FT-IR). The UV-visible spectra revealed a high peak of absorption at 304 nm while SEM analysis revealed the nanoparticles as spherical, irregular, and agglomerated granular structures with average sizes of 59.38, 8.68, and 34.94 nm at 1 µm, 100 nm and 500 nm scales, respectively. EDX profiling verified the presence of magnesium and oxygen and XRD pattern revealed prominent peaks from the crystalline metallic nanoparticles. The FT-IR data demonstrated that fungal biological constituents functioned as reducing or capping agents for the synthesized nanoparticles. The antifungal activity studies against *Alternaria mali,* using poisoned food technique, showed that the nanoparticles notably restrained growth, in a dose-dependent manner. At doses of 0.3%, nanoparticles reduced the mycelial growth up to 1.14 mm, while at 0.2 and 0.1% concentrations showed a growth of 6.11 and 10.81 mm, respectively.

Keywords: *Alternaria mali*, **a**ntimicrobial, apple, magnesium, microscopy, nanoparticles, spectroscopy

INTRODUCTION

The emergence of green nanotechnology encompasses a variety of procedures that minimize the occurrence of poisonous materials for restoring the environment. Microbes that operate as nano-factories include fungi, which possess the innate ability to reduce and oxidize metal ions into metallic or metal oxide nanoparticles (Gade *et al.*, 2010). They are strong enough to withstand ecologically varied settings because of their chemical constitutions. The fungi-mediated synthesis of nanoparticles (NPs) offers a number of benefits over other biological entities including bacteria, plants, and the techniques like physical, chemical, and aerosol processes. The kingdom fungi is incredibly diverse having estimated 1.52 million species. In terms of nutrient cycle and biogeochemical processes, fungi are essential to the web of ecosystem. Perusal of literature has revealed non-availability of information on the mycosynthesis of MgONP's using *Pleurotus sajor-caju*. The present study attempted to study a quick, economical, environmentally friendly, and easily repeatable method for scaling up and easy downstream processing of MgONP's.

Magnesium, an alkaline earth element with oxidation number +2, is required by all the living cells and is vital for regulating important biological polyphosphate compounds including ATP, DNA, and RNA (Lu *et al.*, 2012). Magnesium is necessary for the catalytic activity of hundreds of enzymes. Magnesium is frequently added to fertilizers because it is metallic ion at the core of photosynthetic

pigment chlorophyll (Verbruggen and Hermans, 2013), making it a crucial component of plant growth. MgO is a valuable substance that may be used as a catalyst, to remediate hazardous waste, and as an addition in paints, refractory materials, and superconductor goods (Ma and Bando, 2003).

MgONPs have demonstrated direct and broad-range toxicity towards fungi like *Aspergillus niger* and *Penicillium oxalicum* (Sierra-Fernandez *et al.*, 2017), so are also useful in agriculture (Singh *et al.*, 2019; Rani *et al.*, 2020). The potential of employing several fungal species for the production of MgONPs has not yet fully been realized (Mohanasrinivasan *et al.*, 2018). Apple (*Malus domestica* Borkh.) is the most widely produced commercial fruit crop in the world. The crop is vulnerable to various plant diseases including Alternaria leaf blotch, cankers, and apple scab, with pathogenic fungi responsible for the great majority of them (Muneer *et al.*, 2017; Nabi *et al.*, 2020). Alternaria leaf blotch (ALB), caused by *Alternaria mali*, poses a serious threat to the overall apple productivity and output. ALB has caused massive losses to apple sector in the majority of apple-growing regions worldwide (Filajdic and Sutton, 1991; Cao *et al*., 2024). Nanotechnology offers a practical and safe approach to address plant diseases in both organic and conventional agriculture (Dasgupta *et al.*, 2017; Prasad *et al.*, 2017). Magnesium oxide nanoparticles reportedly are effective against several pathogenic fungi including *Fusarium oxysporum, Alternaria alternata, Rhizopus stolonifera,* and *Mucor plumbeus* (Sawai and Yoshikawa, 2004; Barik *et al.*, 2008; He *et al.*, 2011; Anjum *et al.*, 2023). MgONPs have not been evaluated against *A. mali* till date and in this context, the present study aimed to fabricate MgONPs and evaluate their performance against *A. mali* causing ALB in apple plants.

MATERIALS AND METHODS

This study used a cell-free extract derived from fungal mycelia secretions for biological production of MgONPs using a precursor salt, magnesium nitrate hexahydrate ($Mg(NO_3)_2 \cdot 6H_2O$). Mycogenic synthesis, standardization, characterization of MgONPs and their evaluation against *Alternaria mali* was performed in the Laboratory of Plant Pathology, SKUAST-Kashmir, Shalimar, Srinagar (Kashmir).

Procurement of fungus

For MgONP fabrication, the fungus *Pleurotus sajor-caju* was obtained from the Division of Plant Pathology, SKUAST-Kashmir and sub-cultured at 24±2°C for fresh growth. The culture was then screened for the manufacture of MgONPs using precursor salt magnesium nitrate hexahydrate.

Mycogenic synthesis of MgONPs

P. sajor-caju was grown in 100 mL potato dextrose broth (PDB) medium in 250 mL Erlenmeyer flasks. The culture was grown on a rotary shaker at 150 rpm at 24±2°C for 120 h. Then fungal mycelium was filtered and washed 3 times with double distilled sterilized water. Recovered fungal biomass (15 g) was re-suspended in 100 mL Milli-Q water in 250 mL flask, and shaken at 150 rpm at 24±2°C for 72 h. After incubation, the mycelial mass was filtered through Whatman filter paper No. 1 to obtain cell-free extract. Then 5 mM solution of precursor salt (magnesium nitrate hexahydrate) was prepared in Erlenmeyer flasks using the above cell-free extract. NaOH solution (1 M) was added drop-wise with constant stirring by a magnetic stirrer until alkaline pH (8.0) was achieved. The entire mixture was placed on a magnetic stirrer (500 rpm) at 65±2°C to react with precursor metal salt for 1 h. During reaction time a shift in colour from colourless/transparent to brackish was observed which indicated the synthesis of nanoparticles. The formulation was centrifuged at 10,000 rpm for 30 min, and the resultant pellets washed 2-3 times with milli-Q water to remove the impurities, if any. The pellets were oven-dried at 60°C and stored at 4°C till further use (Sharma *et al.*, 2018).

Characterisation of MgONPs

The samples of bio-transformed MgONPs were examined for their characteristics. UV-visible spectrophotometer (Labtronics) was used in the spectra range of 200 to 800 nm to identify myco-

synthesized MgONPs. The surface or morphological properties of MgONPs such as form and composition were studied using scanning electron microscopy-energy-dispersive X-ray (SEM-EDX) spectroscopy on FE-SEM (Gemini SEM 500, Carl Zeiss, Germany) with a spectral imaging system. MgONPs samples were examined by X-ray diffraction (XRD) on a SmartLab 3kW, RIGAKU, Japan, at 40.0 kV, 30.0 mA, and 2θ values between 20° and 100°, with a flow rate of 2° min^{-1}. The particle size was measured on a particle size analyser (HORIBA SZ-100). Zeta potential of the formulated MgONPs was measured using particle size analyser at 25°C and electrical field strength was around 23.2 V cm^{-1} (Lin *et al.*, 1993). Fourier transform infrared (FTIR) spectroscopy was used to study MgONP formation through functional groups in the fungal extract used. FTIR spectra of a large number of MgONPs were measured using a Perkin Elmer FTIR spectrophotometer following KBr pellet production at room temperature. The range was kept at a resolution of 4 cm^{-1}, between 4000 and 400 cm^{-1}. To determine the biomolecules needed for capping and stabilizing the metal nanoparticles, FTIR analysis was employed. Origin and ImageJ tools were used to identify the quantitative data and acceptable structures.

Mycelial growth inhibition assay

The antimycotic ability of fungal-mediated MgONPs against *Alternaria mali* was evaluated by poisoned food technique (Sharvelle, 1961). Three concentrations of MgONPs (0.1, 0.2 and 0.3%) were tested for their antifungal activity, separately, on potato dextrose agar (PDA) medium. Prior to the experimentation, the fungus was grown on PDA medium in petri plates for 7 days. The PDA medium impregnated with MgONPs was poured into 9 cm dia Petri plates and solidified. Prior to adding, the PDA medium and 5-mm mycelial discs of *A. mali* were taken off the outer margin of a 10 days old culture, and put in the centre of each plate. These petri-plates were then incubated at 24±2^{0}C. An untreated PDA media plates with *A. mali* served as a positive control. The experiment was conducted in a completely randomized design with each treatment, replicated three times. Following a week of incubation, different concentrations of nanoparticles caused different levels of growth inhibition in the fungus. Once the fungus had grown to a full on the control plate, the diameter of colony was evaluated by measuring the mycelial growth in four different directions, and an average was calculated. Vincent's (1947) method was used to compute the percentage of growth inhibition.

$$\text{Growth inhibition (\%)} = \frac{C-T}{C} \times 100$$

Where, C is the average fungal growth in untreated Petri-plates, and T is the average fungal growth in treated/poisoned Petri-plates.

Statistical analysis

Findings of characterization studies were analysed using Origin 9.0 and Image J software, as well as by using conventional statistical tools. Before analysis, the statistical data underwent the necessary adjustments, as recommended by Gomez and Gomez (1984), wherever necessary.

RESULTS AND DISCUSSION

Mycogenic synthesis and characterization of MgONPs

A reaction was allowed by leaving the cell-free fungal extract and the metal salt solution on a magnetic stirrer at 40-50°C for 1 h. The metal salt solution gradually turned brackish after the addition of fungal extract, which was a sign that MgONPs were being synthesized in the solution. The presence of MgO-NPs was confirmed by a small colour shift in the reaction mixtures due to surface plasmon resonance.

UV-visible spectrum of MgONPs

The UV-vis spectra of MgONPs were obtained in the 200-800 nm wavelength range. The MgONPs produced from *P. sajor-caju* exhibited a surface plasmon resonance wavelength of 304 nm in the ultra violet-visible spectrum (Fig. 1). The appearance of individual peaks in UV-vis spectra indicates that the

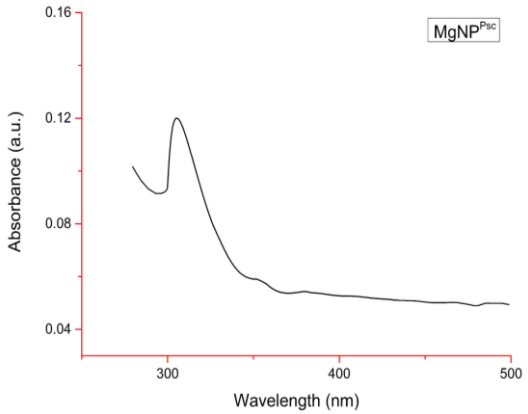

Fig. 1: UV-visible spectrum of MgONPs synthesized from *Pleurotus sajor-caju*

nanoparticles produced are iso-morphological (Jeevanandams *et al.*, 2017). The features of MgONPs may be linked to the efficient capping capability of the bioactive components of fungal extract, as well as ultraviolet (UV) radiation passing through the test sample, which enhanced particle dispersion and homogeneity (Essien *et al.*, 2020).

SEM analysis of MgONPs

Based on the SEM analysis, MgONPs were predicted to have an uneven appearance and can be visualized as angular and irregular shape (Fig. 2). The nanoparticles showed an average size of 59.38, 8.68 nm and 34.94 nm at 1 µm, 100 nm and 500 nm scale, respectively (Fig. 3). The SEM

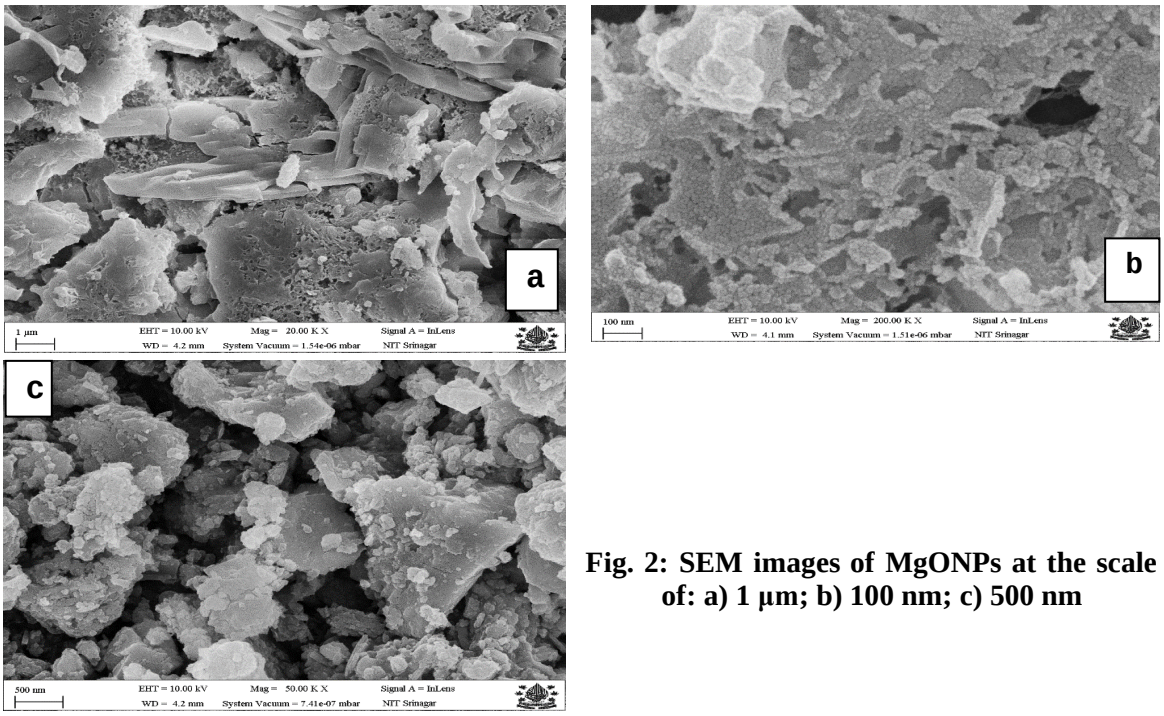

Fig. 2: SEM images of MgONPs at the scale of: a) 1 µm; b) 100 nm; c) 500 nm

pictures show agglomerated structures which suggest the presence of organic waste in the sample. The agglomeration might be attributed to small Van der Waal forces and other interactions inside the nanoparticles (Essien Pugazhendhi *et al.*, 2019; Essien *et al.*, 2020).

EDX analysis MgONPs

The production of MgONPs was observed by EDX examination where atomic weight of oxygen was found to be 80.6%, but its present weight is 73.2%. In tandem, the atomic weight of magnesium was 19.4%, whereas its present weight is 26.8%. The EDX profile provides evidence of MgONPs. Fig. 4 shows the peaks identified during MgONP study.

XRD of MgONPs

The XRD peaks confirmed the crystalline nature of the MgONPs. The diffraction patterns exhibited by exhibited by the nanoparticles ranged from 20 to 70º. Peak diffraction patterns of the material show a conventional constitution with multiple peaks, suggesting Mg at $2\theta = 20.61^{\circ}, 20.61^{\circ}, 21.81^{\circ}, 24.60^{\circ},$

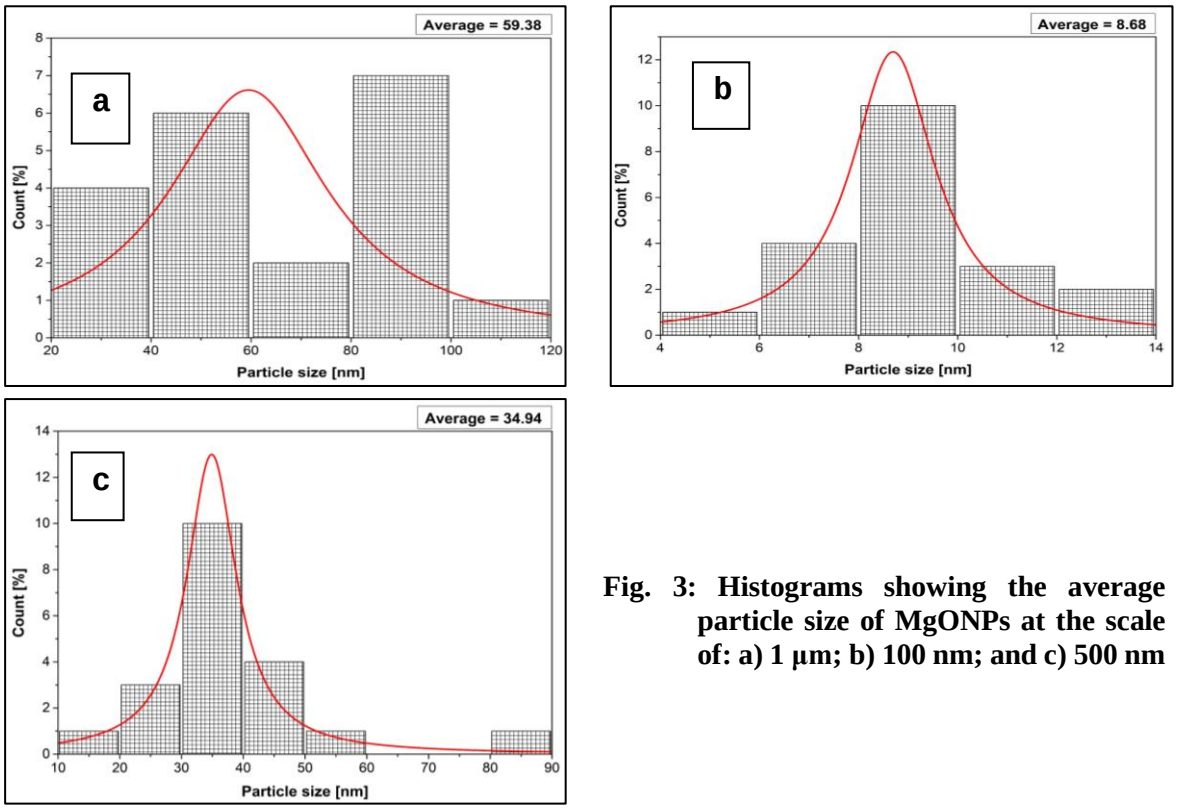

Fig. 3: Histograms showing the average particle size of MgONPs at the scale of: a) 1 µm; b) 100 nm; and c) 500 nm

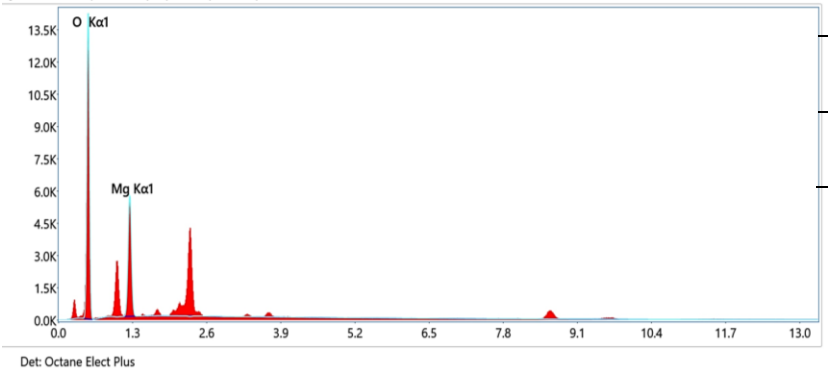

Element	Weight %	Atomic %
O K	59.1	68.7
Mg K	40.9	31.3

Fig. 4: EDX spectrum showing the composition of MgONPs synthesized from *Pleurotus sajor-caju*

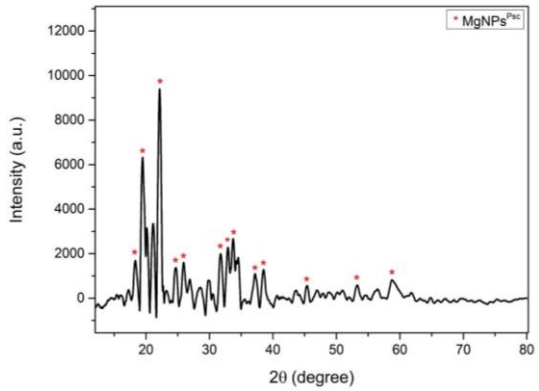

Fig. 5: XRD pattern of MgONPs synthesized from *Pleurotus sajor-caju*

24.54◦, 25.86◦, 28.60◦, 28.60◦, 32.34◦, 33.93◦, 37.15◦, 37.47◦, 64.25◦, 57.74◦, 46.51◦ and 40.50◦. The peak expansion in steady XRD pattern is the consequence of particle size. Applying Bragg's law to the diffraction patterns achieved, the d-spacing in between the planes of crystal were also evaluated. Each value estimated is shown in Table 1 and XRD patterns are displayed in Fig. 5. All diffraction peaks were easily linked to different crystalline planes within the cubic phase MgO (Taleatu *et al.*, 2014).

Particle size analysis (PSA) of MgONPs

The average particle size was obtained by particle size analyzer (PSA). The material was dispersed

Table 1: Values of MgONPs obtained through XRD analysis

2θ	Θ	d-spacing (Å)
20.61	10.30	4.31
20.61	10.30	4.31
21.03	10.51	4.22
21.81	10.91	4.07
24.60	12.30	3.62
24.54	12.27	3.62
25.86	12.93	3.44
28.60	14.30	3.12
28.60	14.30	3.12
28.60	14.30	3.12
32.34	16.17	2.77
33.93	16.96	2.64
37.15	18.58	2.42
37.47	18.74	2.40
64.25	32.13	1.45
57.74	28.87	1.60
46.51	23.26	1.95

Where symbol θ represents 'theta'

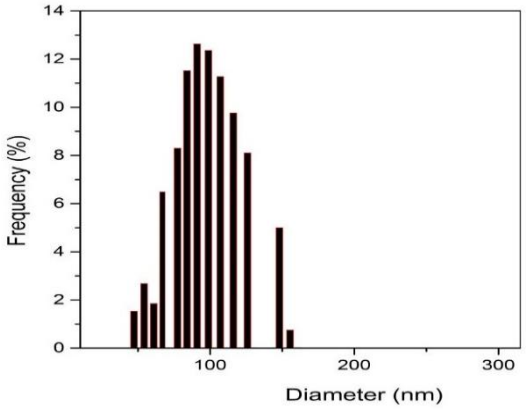

Fig. 6: PSA pattern of MgONPs synthesized from *Pleurotus sajor-caju*

completely in distilled water using ultra-sonicator. The PSA investigation of precipitation showed that it consisted of MgO particles, whose diametric average is 83.85 nm. The higher the temperature, the higher will be the reaction rates. Large amounts of nanoparticles were synthesized in a limited period of time, thus repressing the agglomeration of crystals (Rao *et al.*, 2014). The average surface area (m^2 g^{-1}) of nanoparticles was 83.64 nm. Fig. 6 shows the histograms of dispersed nanoparticles. The polydispersity index (PDI) value of MgONPs (0.31) supports the UV-visible and SEM results which showed MgONPs of various shapes and sizes (Bhattacharjee, 2016). The existence of oxygen atoms on the magnesium oxide surface may be the cause of these negative potentials (Jeevanandam *et al*., 2017). The Zeta potential of -6.91 mV depicts that the nano-formulation has weak electrostatic repulsion, making it prone to aggregation. Surfactants can be used in this case for the application of these nanoparticles in agriculture as they play a crucial role in stabilizing nanoparticles by increasing their stability in aqueous phases through hydrophobic interactions or supercharging effects and reducing surface tension, thereby preventing aggregation (Morsy, 2014; Xu *et al*., 2022).

FT-IR analysis of MgONPs

The FT-IR spectra of MgONPs revealed peaks at 599.47 cm^{-1} and 845.24 cm^{-1}, suggesting MgONP formation. The signal at 3256.11 cm^{-1} indicates a strong O-H bond in water, which supports prior results. The MgONP absorption peaks at 2967.92 cm^{-1} and 2322.05 cm^{-1} correspond to C-H band and C-C stretching of alkane molecules, respectively. The peaks at 1430.41 cm^{-1} and 1085.16 cm^{-1} indicate C=O bonds. Fig. 7 depicts the FT-IR spectroscopy profile of MgONPs, which identified the potential biomolecules in the fungal extract of *P. sajor-caju*. The findings align with studies which demonstrated the significant FT-IR transmission peaks induced by MgO vibrations (Tamilselvi *et al.*, 2013; Mohsen *et al.*, 2020). These changes in MgO vibrations could be related to the fundamental interactions with the organic groups of fungal extracts or the utilisation of precursor salt. Shifts might be ascribed to chemical oxidation or reduction during nanoparticle production (Emmanuel *et al.*, 2015). The presence of bioactive compounds was shown by FT-IR spectra which were hypothesized to reduce or cap the components of MgONPs (Ahmad and Rajgopal, 2015). Various studies have indicated that MgONPs have a high potential for use in agriculture as a new, safe, and environmentally friendly method of plant disease prevention (Andreadelli *et al.*, 2021).

Effect of MgONPs on Alternaria mali in vitro

MgONPs used @ 0.1, 0.2, and 0.3% inhibited the fungal growth, however the activity varied as per the concentration. The fungal mycelial growth was measured as 1.14 mm at the highest concentration (0.3%), 6.11 mm at 0.2%, and 10.81 mm at 0.1%, thus depicting decease in mycelial growth with increase

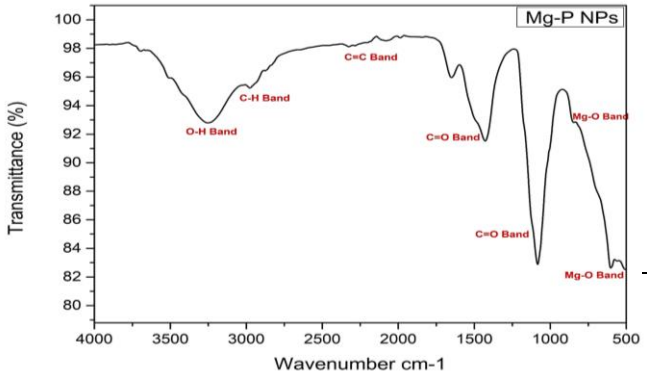

Characteristic vibrations (Functionality)	Wave numbers (cm^{-1})
O-H	3100-3500
C-H	2500-3000
C=C	2000-2500
C=O	1000-2000
C-N	800-1000
Mg-O	500-700

Fig. 7: FT-IR spectra of MgONPs synthesized from *P. sajor-caju*

in nanoparticle concentration. The fungal extract of *P. sajor-caju* also showed a decrease in mycelial growth (15.85 mm) as compared to the control (24.56 mm). Metal salts were more effective with increase in concentration. At 500 ppm, the metal salt was most effective (mycelial growth = 14.78 mm than the fungal extract. Table 2 shows the suppression of *A. mali* by nanoparticle use. The antagonistic effects of MgO NPs on a variety of pathogenic fungi has previously been reported (Dizaj *et al.*, 2014; Yu *et al.*, 2016; Baranwal *et al.*, 2018; Alavi *et al.*, 2019).

Table 2: Effect of treatments on mycelial growth of *Alternaria mali*

Treatments	Concentration (%)	Mean mycelial growth (mm)	SD	SE
FE	100	15.85	0.52	0.30
MgO NPs	0.1	10.81	0.18	0.10
MgO NPs	0.2	6.11	0.24	0.14
MgO NPs	0.3	1.14	0.07	0.04
MS	300 ppm	21.63	0.35	0.20
MS	500 ppm	14.78	0.29	0.17
Control	-	24.56	0.37	0.21

FE = Fungal extract (*P. sajor-caju*); MS = Metal salt; SD = Standard deviation; SE = Standard error

Conclusion: In present study, the myco-assisted production of MgONPs utilizing *P. sajor-caju* extract is reported. The aqueous extract contains organic compounds that function as stabilizing and reducing agents. UV, SEM, EDX, XRD and FT-IR analysis were employed to characterize the MgONPs. The strong absorption peaks of the nanoparticles indicate their fabrication as MgONPs. The functional groups of *P. sajor-caju* filtrate, acting as stabilizing and reducing agents, produce MgONPs which are spherical in shape, angular and nanoscale size. The antifungal properties of MgONPs were tested using the poisoned food technique. As a result of their excellent antimicrobial properties, myco-synthesized MgONPs could potentially be employed to control Alternaria leaf blotch in apple. To further analyse any possible hazardous consequences of MgONPs, supplementary research is required to determine the toxicity of myco-heck in field conditions. Further advanced studies on possible toxic effects of fungal extract-assisted MgONPs is suggested.

Conflict of interest: The authors declare having no conflicting interests.

REFERENCES

Ahmad, H. and Rajgopal, K. 2015. Pharmacology of *Pterocarpus marsupium* Roxb. *Journal of Medicinal Plants Research*, **5**(3). [*https://doi.org/10.5376/mpr.2015.05.0003*].

Alavi, M., Karimi, N. and Salimikia, I. 2019. Phytosynthesis of zinc oxide nanoparticles and its antibacterial, antiquorum sensing, antimotility, and antioxidant capacities against multidrug resistant bacteria. *Journal of Industrial and Engineering Chemistry*, **72**: 457-473.

Andreadelli, A., Petrakis, S., Tsoureki, A., Tsiolas, G., Michailidou, S., Baltzopoulou, P., *et al*., 2021. Effects of magnesium oxide and magnesium hydroxide microparticle foliar treatment on tomato pr gene expression and leaf microbiome. *Microorganisms*, **9**(6): 1217. *[https://doi.org/10.3390/microorganisms9061217]*.

Anjum, S., Vyas, A. and Sofi, T.A. 2023. Fungi-mediated synthesis of nanoparticles: Characterization process and agricultural applications. *Journal of the Science of Food and Agriculture*, **103**(10): 4727-4741.

Baranwal, A., Srivastava, A., Kumar, P., Bajpai, V.K., Maurya, P.K. and Chandra, P. 2018. Prospects of nanostructure materials and their composites as antimicrobial agents. *Frontiers in Microbiology*, **9**: 309-424.

Barik, T.K., Sahu, B. and Swain, V. 2008. Nanosilica - From medicine to pest control. *Parasitolology Research*, **103**: 253-258.

Bhattacharjee, S. 2016. DLS and zeta potential – What they are and what they are not? *Journal of Controlled Release*, **235**: 337-351.

Cao, C., Gong, S., Li, Y., Tang, J., Li, T., and Zhang, Q. 2024. Pathogenic factors and mechanisms of the Alternaria leaf spot pathogen in apple. *Horticulturae*, **10**(3): 212. [*https://doi.org/10.3390/horticulturae10030212*].

Dasgupta, N., Ranjan, S. and Ramalingam, C. 2017. Applications of nanotechnology in agriculture and water quality management. *Environmental Chemistry Letters*, **15**: 591-605.

Dizaj, S.M., Lotfipour, F., Barzegar-Jalali, M., Zarrintan, M.H. and Adibkia, K. 2014. Antimicrobial activity of the metals and metal oxide nanoparticles. *Materials Science and Engineering: C*, **44**: 278-284.

Emmanuel, R., Palanisamy, S., Chen, S.M., Chelladurai, K., Padmavathy, S., Saravanan, M., *et al.*, 2015. Antimicrobial efficacy of green synthesized drug blended silver nanoparticles against dental caries and periodontal disease causing microorganisms. *Materials Science and Eng*ineering, **56**: 374-379.

Essien Pugazhendhi, A., Prabhu, R., Muruganantham, K., Shanmuganathan, R. and Natarajan, S. 2019. Anticancer, antimicrobial and photocatalytic activities of green synthesized magnesium oxide nanoparticles (MgO NPs) using aqueous extract of *Sargassum wightii*. *Journal of Photochemistry and Photobiology B: Biology*, **190:** 86-97.

Essien, R., Astasie, V.N., Okeafor, A.O. and Nwude, D.O. 2020. Biogenic synthesis of magnesium oxide nanoparticles using *Manihot esculenta* (Crantz) leaf extract. *International Nano Letters*, **10**(1): 43-48.

Filajdic, N. and Sutton, T.B. 1991. Identification and distribution of *Alternaria mali* on apples in North Carolina and susceptibility of different varieties of apples to Alternaria blotch. *Plant Disease*, **75**: 1045-1048.

Gade, A., Ingle, A., Whitely, C. and Rai, M. 2010. Mycogenic metal nanoparticles: progress and applications. *Biotechnology Letters*, **32**: 593-600.

Gomez, K.A. and Gomez, A.A. 1984. *Statistical Procedures for Agricultural Research*. John Wiley & Sons, New York, USA.

He, L., Liu, Y., Mustapha, A. and Lin, M. 2011. Antifungal activity of zinc oxide nanoparticles against *Botrytis cinerea* and *Penicillium expansum*. *Microbiological Research*, **166**(3): 207-215.

Jeevanandams, J., Chan, Y.S. and Danquah, M.K. 2017. Biosynthesis and characterization of MgO nanoparticles from plant extracts via induced modified nucleation. *New Journal of Chemistry*, **41**(7): 2800-2814.

Lin, W., Coombes, A.G.A., Davies, M.C., Davis, S.S. and Illum, L. 1993. Preparation of sub-100 nm human serum albumin nanoparticles using a pH-coacervation method. *Journal of Drug Target*ing, **1**: 237-243.

Lu, S., Huang, W., Li, X., Huang, Z., Liu, X., Chen, Y., *et al.*, 2012. Insights into the role of magnesium triad in myo-inositol monophosphatase: Metal mechanism, substrate binding, and lithium therapy. *Journal of Chemical Information and Modelling*, **52**(9): 2398-2409.

Ma, R. and Bando, Y. 2003. Uniform MgO nanobelts formed from in situ Mg_3N_2 precursor. *Chemical Physics Letters*, **370**(5-6): 770-773.

Mohanasrinivasan, V., Subathra Devi, C., Mehra, A., Prakash, S., Agarwal, A., Selvarajan, E. *et al.*, 2018. Biosynthesis of MgO nanoparticles using *Lactobacillus* sp. and its activity against human leukemia cell lines HL-60. *BioNanoScience*, **8**: 249-253.

Mohsen, E., Younis, I.Y. and Farag, M.A. 2020. Metabolites profling of Egyptian *Rosa damascena* Mill. flowers as analysed via ultra-high performance liquid chromatography-mass spectrometry and solid-phase micro-extraction gas chromatography-mass spectrometry in relation to its anti-collagenase skin. *Industrial Crops and Products*, **155**: 13. [*https://doi.org/10.1016/j.indcrop.2020.112818*].

Muneer, A.S., Bhat, K.M., Mir, J.I., Mir, M.A., Nabi, S.U., Bhat, H.A., *et al.*, 2017. Phenotypic and molecular screening for disease resistance of apple cultivars and selections against apple scab (*Venturia inaequalis*). *International Journal of Chemical Studies*, **5**(4): 1107-1111.

Morsy, S.M. 2014. Role of surfactants in nanotechnology and their applications. *International Journal of Current Microbiology and Applied Sciences*, **3**(5): 237-260.

Nabi, S.U., Baranwal, V.K., Yadav, M.K. and Rao, G.P. 2020. Association of apple necrotic mosaic virus (ApNMV) with mosaic disease in commercially grown cultivars of apple (*Malus domestica* Borkh) in India. *3 Biotech*, **10**: 1-9. [*https://doi.org/10.1007/s13205-020-2117-6*].

Prasad, R., Bhattacharyya, A. and Nguyen, Q.D. 2017. Nanotechnology in sustainable agriculture: Recent developments, challenges, and perspectives. *Frontiers in Microbiology*, **8**: 1014. [*https://doi.org/10.3389/fmicb.2017.01014*].

Rani, P., Kaur, G., Rao, K.V., Singh, J. and Rawat, M. 2020. Impact of green synthesized metal oxide nanoparticles on seed germination and seedling growth of *Vigna radiata* (mung bean) and *Cajanus cajan* (red gram). *Journal of Inorganic and Organometallic Polymers and Materials*, **30:** 4053-4062.

Rao, K.G., Ashok, C.H., Rao, K.V. and Chakra, C.S. 2014. Structural properties of MgO nano-particles: Synthesized by co-precipitation technique. *International Journal of Science and Research*, **3**(12): 43-46.

Sawai, J. and Yoshikawa, T. 2004. Quantitative evaluation of antifungal activity of metallic oxide powders (MgO, CaO and ZnO) by an indirect conductimetric assay. *Journal of Applied Microbiol*ogy, **96**(4): 803-809.

Sharma, G., Soni, R. and Jasuja, N.D. 2018. Phytoassisted synthesis of magnesium oxide nanoparticles with *Swertia chirayita*. *Journal of Taibah University of Science*, **11**(3): 471-477.

Sharvelle, E.G. 1961. *The Nature and Uses of Modern Fungicides*. Burgers Publication Co., Minneapolis, Minnesota, USA.

Sierra-Fernandez, A., De la Rosa-García, S.C., Gomez-Villalba, L.S., Gómez-Cornelio, S., Rabanal, M.E., Fort, R. *et al.*, 2017. Synthesis, photocatalytic, and antifungal properties of MgO, ZnO and Zn/Mg oxide nanoparticles for the protection of calcareous stone heritage. *ACS Applied Materials & Interfaces*, **9**: 24873-24886. [*https://doi.org/10.1021/acsami.7b06130*].

Singh, J., Kumar, V., Jolly, S.S., Kim, K.H., Rawat, M., Kukkar, D. *et al.*, 2019. Biogenic synthesis of silver nanoparticles and its photocatalytic applications for removal of organic pollutants in water. *Journal of Industrial and Engineering Chemistry*, **80**: 247-257.

Taleatu, B.A., Omotoso, E., Lal, C., Makinde, W.O., Ogundele, K.T., Ajenifuja, E., *et al.*, 2014. XPS and some surface characterizations of electrodeposited MgO nanostructure. *Surface and Interface Analysis*, **46**: 372-377.

Tamilselvi, P., Yelilarasi, A., Hema, M. and Anbarasan, R. 2013. Synthesis of hierarchical structured MgO by sol-gel method. *Nano Bulletin*, **2**: 130106. *[https://doi.org/10.1234/NANO130106]*.

Verbruggen, N. and Hermans, C. 2013. Physiological and molecular responses to magnesium nutritional imbalance in plants. *Plant and Soil*, **368**: 87-99.

Xu, F., Zhong, X., Li, Z., Cao, W., Yang, Y. and Liu, M. 2022. Synergistic mechanisms between nanoparticles and surfactants: Insight into NP–surfactant interactions. *Frontiers in Energy Research*, **10**: 913360. [*https://doi.org/10.3389/fenrg.2022.913360*].

Yu, Q., Li, J., Zhang, Y., Wang, Y., Liu, L. and Li, M. 2016. Inhibition of gold nanoparticles (AuNPs) on pathogenic biofilm formation and invasion to host cells. *Scientific Reports*, **6**(1): 26667. [*https://doi.org/10.1038/srep26667*].